Neurobiology of Aging 75 (2019) 98–108

Contents lists available at ScienceDirect

Neurobiology of Aging

journal homepage: www.elsevier.com/locate/neuaging

Intranasal insulin activates Akt2 signaling pathway in the hippocampus of wild-type but not in APP/PS1 Alzheimer model mice

Sami Gabbouj [a,1], Teemu Natunen [a,1], Hennariikka Koivisto [b], Kimmo Jokivarsi [b], Mari Takalo [a], Mikael Marttinen [a], Rebekka Wittrahm [a], Susanna Kemppainen [a], Reyhaneh Naderi [b,c], Adrián Posado-Fernández [d], Simo Ryhänen [a], Petra Mäkinen [a], Kaisa M.A. Paldanius [a], Gonçalo Doria [d], Pekka Poutiainen [e], Orfeu Flores [d], Annakaisa Haapasalo [b], Heikki Tanila [b,1], Mikko Hiltunen [a,*,1]

[a] Institute of Biomedicine, University of Eastern Finland, Kuopio, Finland
[b] A. I. Virtanen Institute for Molecular Sciences, University of Eastern Finland, Kuopio, Finland
[c] Department of Biology, Shahid Bahonar University, Kerman, Iran
[d] STAB VIDA Lda, Madan Parque, Rua dos Inventores, Caparica, Portugal
[e] Diagnostic Imaging Centre, PET Radiopharmacy, Kuopio University Hospital, Kuopio, Finland

ARTICLE INFO

Article history:
Received 13 July 2018
Received in revised form 2 November 2018
Accepted 12 November 2018
Available online 17 November 2018

Keywords:
Akt2
Alzheimer's disease
FDG-PET
Hippocampus
Homeostatic microglia
Insulin signaling

ABSTRACT

Type 2 diabetes mellitus (T2DM) increases the risk for Alzheimer's disease (AD). Human AD brains show reduced glucose metabolism as measured by [18F]fluoro-2-deoxy-2-D-glucose positron emission tomography (FDG-PET). Here, we used 14-month-old wild-type (WT) and $APP_{Swe}/PS1_{dE9}$ (APP/PS1) transgenic mice to investigate how a single dose of intranasal insulin modulates brain glucose metabolism using FDG-PET and affects spatial learning and memory. We also assessed how insulin influences the activity of Akt1 and Akt2 kinases, the expression of glial and neuronal markers, and autophagy in the hippocampus. Intranasal insulin moderately increased glucose metabolism and specifically activated Akt2 and its downstream signaling in the hippocampus of WT, but not APP/PS1 mice. Furthermore, insulin differentially affected the expression of homeostatic microglia markers *P2ry12* and *Cx3cr1* and autophagy in the hippocampus of WT and APP/PS1 mice. We found no evidence that a single dose of intranasal insulin improves overnight memory. Our results suggest that intranasal insulin exerts diverse effects on Akt2 signaling, autophagy, and the homeostatic status of microglia depending on the degree of AD-related pathology.

1. Introduction

It is well established that type 2 diabetes mellitus (T2DM) increases the risk for Alzheimer's disease (AD) (Irie et al., 2008; Liu et al., 2011; Vanhanen and Soininen, 1998; Xu et al., 2009). Several postmortem studies have revealed insulin resistance in the AD brain (Liu et al., 2011; Steen et al., 2005) and led to the suggestion that AD represents a "type 3" diabetes mellitus (Steen et al., 2005). T2DM has been associated with brain atrophy in the regions strongly affected in AD, including hippocampus (Moran et al., 2013). Furthermore, based on longitudinal studies, it has been estimated that the rate of global brain atrophy is even 3 times faster in patients with T2DM than in healthy elderly individuals (Kooistra et al., 2013; van Elderen et al., 2010), suggesting that impaired insulin signaling is adversely linked to neurodegeneration. Apart from regulating glucose metabolism in the brain, insulin acts as a neurotrophic factor and thereby may contribute to neuronal development and plasticity (Chiu et al., 2008). One of the key players in insulin signaling is the Akt family of serine/threonine kinases, whose downstream signaling has been associated with crucial physiological functions of the brain, such as promotion of dendritic spine and synapse formation (Lee et al., 2011). Furthermore, insulin/Akt signaling is linked to the regulation of hyperphosphorylation of

* Corresponding author at: Professor of Tissue and Cell Biology, Institute of Biomedicine, University of Eastern Finland, P.O. Box 1627, Kuopio FI-70211, Finland. Tel.: +358 40 3552014; fax: +358 17 162 131.
E-mail address: mikko.hiltunen@uef.fi (M. Hiltunen).
[1] Equal contribution.

https://doi.org/10.1016/j.neurobiolaging.2018.11.008

tau via glycogen synthase kinase 3β (GSK3β) (Hooper et al., 2008). The Akt family comprises Akt1, Akt2, and Akt3, of which the last is the least well characterized and mainly involved in brain development (Alcantara et al., 2017). The downstream signaling of Akt1, Akt2, and Akt3 is activated upon phosphorylation by mechanistic target of rapamycin complex 2 (mTORC2) at the serine 474, 473, and 472 sites, and by 2-phosphoinositide-dependent kinase 1 (PDK1) at the threonine 309, 308, and 305 sites, respectively (Noguchi and Suizu, 2012). Phosphorylation of both serine and threonine residues is required to fully activate each Akt isoform. However, the distinctive roles of each phosphorylation site remains to be elucidated (Noguchi and Suizu, 2012).

Reduced glucose metabolism in the parietal cortex as measured by fluorodeoxyglucose positron emission tomography (FDG-PET) is 1 of the key brain imaging findings in patients with AD (Cohen and Klunk, 2014). Reduced glucose metabolism in the posterior cingulate cortex and hippocampus can be observed years before the onset of dementia and is associated with increased risk of AD (Mosconi et al., 2006). Intriguingly, similar impairment in regional glucose metabolism to that in the AD brain has been reported in subjects with T2DM (Baker et al., 2011). Although most of the brain glucose uptake is based on insulin-independent glucose transporter subtypes 1 and 3 (Shah et al., 2012), the insulin-dependent glucose transporter 4 is present in certain brain regions, most notably in the hippocampus (Vannucci et al., 1998). Based on these findings, increasing brain insulin levels appears as a rational potential treatment for AD. However, to allow successful utilization of this treatment approach, 2 major challenges need to be overcome. First, the blood-brain barrier limits the passage of systemically administered insulin into the forebrain (Dhuria et al., 2010), although it can relatively freely access the hypothalamus (Ganong, 2000). Second, peripheral administration of insulin automatically leads to hypoglycemia. As demonstrated by animal studies, intranasally administered insulin has access deep into the brain along the olfactory and trigeminal pathways and reaches the brain at therapeutic concentrations (Chapman et al., 2017). Although intranasal insulin transiently raises serum insulin levels and lowers plasma glucose levels within the normal physiological range, these transient effects are considerably less problematic than the sustained increases caused by peripheral delivery of insulin (Chapman et al., 2017). Studies in cognitively healthy humans have shown encouraging results, which indicate that intranasal insulin may improve cognition in a dose-dependent and memory task–dependent manner without major adverse effects (Benedict et al., 2004, 2007, 2008; Brünner et al., 2015; Chapman et al., 2017; Novak et al., 2014). Also clinical trials in individuals with mild cognitive impairment and patients with AD suggest that both acute and chronic administration of intranasal insulin ameliorate multiple aspects of cognition, including verbal memory, memory storage, and selective attention (Craft et al., 2012; Reger et al., 2006, 2008). Cognitively impaired patients also exhibit functional improvement after treatment with intranasal insulin (Craft et al., 2012; Reger et al., 2008). However, although patients not carrying the apolipoprotein E ε4 (*APOE* ε4) allele mostly benefitted from intranasal insulin treatment (Craft et al., 2012; Reger et al., 2008, 2006), the treatment of *APOE* ε4 allele carriers has yielded mixed responses (Chapman et al., 2017). Intranasal insulin treatment has also been shown to alter the levels of AD biomarkers in the blood and cerebrospinal fluid (Chapman et al., 2017). A number of animal studies on the effects of intranasal insulin on the hallmark AD brain pathologies and cognitive impairment have generally demonstrated promising results (Chapman et al., 2017). Both acute and repetitive intranasal insulin administration have been reported to improve spatial and object recognition memory, motor learning, and decision-making of wild-type (WT), senescence-accelerated SAMP8, and AD model mice (3xTG) (Apostolatos et al., 2012; Chapman et al., 2017; Mao et al., 2016; Salameh et al., 2015). There are also some studies that do not indicate improvements in memory tests after intranasal insulin treatment in mice (Bell and Fadool, 2017), but such studies are in the minority. Apart from these aforementioned effects, it is expected that intranasal insulin may modulate the function of glia because insulin deficit has been linked to AD-associated neuroinflammation (Zhao and Townsend, 2009). This is a particularly relevant and timely issue given the recent characterization of a unique type of microglia associated with neurodegenerative diseases (disease-associated microglia [DAM]) and characterized by specific RNA profiles (Keren-Shaul et al., 2017). Importantly, DAM have the potential to restrict neurodegeneration, which emphasizes the need for assessing the RNA signature of DAM targets on different treatment procedures, which are aimed to modify AD-associated outcome measures.

Here, we have addressed the effect and mechanisms of intranasal insulin treatment in the well-characterized $APP_{Swe}/PS1_{dE9}$ (APP/PS1) transgenic AD mouse model (Borchelt et al., 1997). APP/PS1 mice develop peripheral glucose intolerance, but not insulin resistance, nor hyperinsulinemia (Hiltunen et al., 2012; Stanley et al., 2016; Takalo et al., 2014). Previous studies in APP/PS1 and APP23 mice, which carry the same APP_{Swe} mutation, have shown that this AD genotype predisposes to insulin resistance but requires another triggering factor, such as the overexpression of insulin-like growth factor 2 (Hiltunen et al., 2012; Takalo et al., 2014), knockdown of leptin (Takeda et al., 2010), or high-fat diet (Hiltunen et al., 2012) to develop insulin resistance. Although the role of insulin signaling along the Akt pathway in the brain has previously been investigated, no studies have yet elucidated the distinctive responses of the Akt1 and Akt2 signaling pathways in different brain areas with respect to insulin treatment. Here, we demonstrate that intranasal insulin treatment increases glucose metabolism in the ventral brain areas and hippocampus of WT mice, but a similar increase is not detected in APP/PS1 mice. We also show that intranasal insulin specifically activates Akt2 and its downstream signaling and differentially affects the expression of homeostatic microglia and autophagy markers in the hippocampus of WT and APP/PS1 mice.

2. Material and methods

2.1. Animals

Fourteen-month-old male $APP_{Swe}/PS1_{dE9}$ (APP/PS1) mice (n = 17) and their age-matched WT littermates were used in the study (n = 15). In total, these 32 mice were used during the study. However, a different number of these mice were used in each analysis as indicated in their corresponding methods section. The APP/PS1 colony founders were obtained from D. Borchelt and J. Jankowsky (Johns Hopkins University, Baltimore, MD, USA), while the mice were raised locally at the Laboratory Animal Center in Kuopio, Finland. Mice were created by co-injection of chimeric mouse/human APP_{Swe} and human PS1-dE9 (deletion of exon 9) vectors controlled by independent mouse prion protein promoter elements. The 2 transgenes co-integrated and co-segregate as a single locus (Jankowsky et al., 2004). Mice were backcrossed to C57BL/6J for 21 generations. The mice were kept in a controlled environment (constant temperature, 22 ± 1 °C, humidity 50%–60%, lights on 07:00–19:00) and had food and water available ad libitum. All animal procedures were carried out in accordance with the guidelines of the European Community Council Directives 86/609/EEC and approved by the Animal Experiment Board of Finland.

2.2. Treatment

Mice were treated intranasally with natural insulin (Humulin, 100 U/mL; Eli Lilly, Indianapolis, IN, USA) according to the protocol described by Hanson et al. (2013) at a total dose of 30 μL (3.0 U) per animal (Hanson et al., 2013). First, the mice were handled daily for 5 days. During the next week, the mice were familiarized with intranasal application of saline for another 5 days. The first intranasal application for a PET imaging session took place on the following day. The second PET session a week later was also preceded by a practice day with intranasal saline. The mouse was gently held supine on a towel, and a droplet of 3 μL insulin was administered using a pipette into each nostril at a time. The mouse was kept supine for 30 seconds after each administration and then let to walk for 1 minute before the following administration. The same cycle was repeated until the desired total dose was reached. Alternatively, mice were administered 0.9% saline according to the same protocol.

2.3. PET imaging

In total, 11 APP/PS1 and 11 WT littermate mice were used in [^{18}F] fluoro-2-deoxy-2-D-glucose (FDG) PET study to assess potential genotype differences and insulin effects on brain glucose uptake. The animals were imaged using a dedicated PET scanner (Inveon DPET; Siemens Healthcare, Erlangen, Germany), followed immediately by computed tomography analysis (Flex SPECT/CT; Northridge Trimodality Imaging, Chatsworth, CA, USA) for anatomical reference images using the same animal holder. The mice were placed on a heated animal holder on the scanner bed in a prone position and secured with adhesive tape to prevent movement during scanning. Each animal underwent PET imaging twice with 1 week between the sessions. Mice were fasted 5–7 hours before the imaging. The mice received either insulin or saline intranasally in a counterbalanced order 4 hours before the imaging session. For anesthesia during imaging, 2% isoflurane was used with N_2/O_2 flow (70%/30%) through a facemask. Dynamic imaging of 110 minutes was started at the time of the administration of (10.49 ± 0.4) MBq of FDG that was administered through the tail vein. Data were gathered in list-mode form; corrected for dead-time, randoms, scatter, and attenuation; and reconstructed with 2D-OSEM. Regions of interest were drawn for olfactory bulb, whole ventral brain, hippocampus and cerebellum, and heart as a reference using Carimas 2.9 software (Turku PET Centre, Finland). The accumulated activity data were normalized to the accumulated activity in the heart. The time window from 40 to 110 minutes after injection was chosen for further analysis.

2.4. Behavioral testing

Some mice (7 APP/PS1 and 4 WT) could not be accepted to the swim test because of wounds in the tail after repeated injections. They were replaced by available male mice of the corresponding genotype and age (6 APP/PS1 and 4 WT). Thus, 10 APP/PS1 and 11 WT mice were included in the behavioral testing. Spatial learning and memory were assessed in the Morris swim task. The test was conducted in a white circular wading pool (diameter 120 cm) with a transparent submerged platform (diameter 14 × 14 cm) 1.0 cm below the surface serving for escape from the water. The pool was open to landmarks in the room (white screen blocking the view to the computer and the experimenter, green water hose, door, 1-m high black pattern on the wall). Temperature of the water was kept at 20 ± 0.5 °C. The acquisition phase was preceded by 2 practice days with a guiding alley to the platform (day-4 and day-3, not shown). During the acquisition phase (days 1–5), the location of the hidden platform was kept constant (SE quadrant) and the starting position varied between 4 different locations at the pool edge, with all mice starting from the same position in a given trial. Each mouse was placed in the water with its nose pointing toward the pool wall. If the mouse failed to find the escape platform within 60 seconds, it was placed on the platform for 10 seconds by the experimenter (the same time was allowed for mice that found the platform). The acquisition phase consisted of 5 daily trials with a 10-minute intertrial interval. The mice received no treatment during the acquisition phase. On day 8, the platform was placed in a new location (NW, different distance from the pool wall), and 5 trials were run as before. After the last trial, the mice received intranasally either insulin or saline and were returned to their home cage. On day 9 (24 hours after treatment), a probe trial of 60 seconds was run without the platform to determine the search bias as an index of spatial memory. On day 13, the platform was placed in a new location (NE), and 5 acquisition trials were run as before. After the last trial, the mice that previously received insulin were given saline intranasally and vice versa. On day 14, the search bias was tested in a 60-second probe trial without the platform. The experimenter was blind to the genotype and treatment of the mice. The mouse was video-tracked, and the video analysis program calculated the escape latency, swimming speed, path length and time in the pool periphery (10 cm from the wall), and the platform zone (diameter 30 cm).

2.5. Sample preparation

At the end of the study, all but 1 mouse from those that underwent PET imaging (with or without behavioral testing, 10 APP/PS1 and 11 WT mice) were treated once more with either intranasal insulin or saline. Two hours later, the mice were deeply anesthetized with pentobarbiturate-chloralhydrate cocktail and transcardially perfused with ice-cold saline for 3 minutes to rinse blood from the brain. The brains were removed, and hippocampi and olfactory bulb were dissected on ice and snap-frozen in liquid nitrogen. The samples were stored at −70 °C. Olfactory bulb and hippocampus tissue samples were collected into microcentrifuge tubes and weighed. Samples were homogenized in 250 μL of phosphate-buffered saline (DPBS; Lonza) using a stirrer. Fractions of homogenates were taken to RNA isolation (50 μL of homogenate and 500 μL Trizol) and Western blot analysis (100 μL of homogenate was supplemented with protease inhibitors and phosphatase inhibitors 1:100; Thermo Scientific). The remaining 100 μL of homogenate was left unprocessed and stored at −80 °C.

2.6. Western blot analysis

The inhibitor-supplemented total protein fractions were further diluted by taking 50 μL of homogenate and adding 70 μL of T-PER Tissue Protein Extraction Reagent (Thermo Scientific). After incubating for 20 minutes on ice, samples were centrifuged for 10 minutes at 16,000 × *g*, and the supernatant was transferred into a new microcentrifuge tube. Protein concentrations were measured using the Pierce BCA Protein Assay Kit (Thermo Scientific); 10–20 μg of total protein lysates were separated by SDS-PAGE using NuPAGE 4%–12% Bis-Tris Midi Protein Gels (Thermo Scientific) and subsequently transferred to polyvinylidene difluoride membranes using the iBlot 2 Dry Blotting System (Thermo Scientific). Unspecific antibody binding was prevented by incubating the blots in blocking solution containing 5% nonfat milk or 5% bovine serum albumin (BSA) in 1x Tris-buffered saline with 0.1 % Tween 20 (TBST) for 1 hour at room temperature. Proteins were detected from the blots using the following primary antibodies diluted in the appropriate ratio with 1x TBST and incubated overnight at +4 °C: rabbit anti-

phospho-Akt1 (Ser473, 1:1000, #9018; Cell Signaling Technology), rabbit anti-phospho-Akt2 (Ser474, 1:1000, #8599; Cell Signaling Technology), rabbit anti-phospho-Akt (Thr308/309/305, 1:1000, #13038; Cell Signaling Technology), rabbit anti-Akt1 (1:1000, #75692; Cell Signaling Technology), rabbit anti-Akt2 (1:1000, #3063; Cell Signaling Technology), rabbit anti-Akt (1:1000, #9272; Cell Signaling Technology), rabbit anti-phospho-GSK3β (Ser9, 1:1000, #9336; Cell Signaling Technology), rabbit anti-GSK3β (1:1000, #9315; Cell Signaling Technology), custom-made mouse anti-phospho-tau detecting the Ser202, Thr205, and Ser208 residues (B6, 1:1000), mouse anti-4R-Tau (RD4, 1:1000, 05-804; Millipore), mouse anti-SQSTM1/p62 (1:1000, #5114; Cell Signaling Technology), mouse anti-LC3 (1:1000, ab51520), and mouse anti-GAPDH (1:15,000, ab8245; Abcam). Blots were subsequently probed with the appropriate horseradish peroxidase (HRP)–conjugated secondary antibodies, either sheep anti-mouse-HRP (1:5000, NA931V; GE Healthcare) or donkey anti-rabbit-HRP (1:5000, NA934V; GE Healthcare) diluted in 1x TBST and incubated for 1 hour at room temperature. Enhanced chemiluminescence (GE Healthcare) was used to detect the protein bands. Blots were imaged with the ChemiDoc MP system (Bio-Rad), and images were quantified using the Image Lab (Bio-Rad) software.

2.7. Real-time quantitative PCR analysis

RNA was isolated from homogenates using the Direct-zol RNA MiniPrep (Zymo Research). RNA concentrations were measured using the NanoDrop ND-1000 spectrophotometer (Thermo Scientific). Total of 250 ng of RNA was subsequently synthesized into cDNA using the Transcriptor First Strand cDNA Synthesis Kit (Roche). Real-time quantitative PCR (RT-qPCR) was subsequently run using the LightCycler 480 Instrument II (Roche) with the LightCycler 480 SYBR Green I Master (Roche) and the following primers: mouse *Rictor* forward 5′-AGT CTG AGT ACC GTG GTA AG-3′, mouse *Rictor* reverse 5′-CTT TCA TAA ACC TGC TTG GC-3′, mouse *Sesn3* forward 5′-TTT GGT AGT GGC ATC AAT CC-3′, mouse *Sesn3* reverse 5′-TCC ACA ATC CCA AAG TTG C-3′, mouse *Pak1* forward 5′-ACC ACT TCC TGT TAC TCC AA-3′, mouse *Pak1* reverse 5′-ACA CTC ACT ATG CTC CGT AA-3′, mouse *P2ry12* forward 5′-GCT TGG CAA CTC ACC TTC AC-3′, mouse *P2ry12* reverse 5′-AGG CAG CCT TGA GTG TTC TTC-3′, mouse *Cx3cr1* forward 5′-CGT GAG ACT GGG TGA GTG AC-3′, mouse *Cx3cr1* reverse 5′-CAG ACC GAA CGT GAA GAC GA-3′, mouse *Trem2* forward 5′-TGG AAC CGT CAC CAT CAC TC-3′, mouse *Trem2* reverse 5′-TGG TCA TCT AGA GGG TCC TCC-3′, mouse *Tyrobp* forward 5′-ACC CGG AAA CAA CAC ATT GC-3′, mouse *Tyrobp* reverse 5′-TTG CCT CTG TGT GTT GAG GT-3′, mouse *Cst7* forward 5′-GTG AAG CCA GGA TTC CCC AA-3′, mouse *Cst7* reverse 5′-AAC AGG CCT CAG CAG AAT CG-3′, mouse *Bdnf* forward 5′-TGG CTG ACA CTT TTG AGC AC-3′, mouse *Bdnf* reverse 5′-GTT TGC GGC ATC CAG GTA AT-3′, mouse *Gfap* forward 5′-GCA CTC AAT ACG AGG CAG TG-3′, mouse *Gfap* reverse 5′-GGC GAT AGT CGT TAG CTT CG-3′, mouse *Gapdh* forward 5′-GAA GGT CGG TGT GAA CGG AT-3′, and mouse *Gapdh* reverse 5′-TTC CCA TTC TCG GCC TTG AC-3'. Results were calculated using the $2^{-\Delta\Delta Ct}$ method (Livak and Schmittgen, 2001).

2.8. Statistics

IBM SPSS, versions 21 and 23, were used to analyze the data. The PET data were analyzed using the paired-sample *t*-test. The acquisition phase of the Morris swim task was analyzed with the analysis of variance (ANOVA) for repeated measures (ANOVA-RM) using day as the within-subject factor and genotype as the between-subjects factor. Spatial search bias during the probe trials was analyzed with ANOVA-RM using treatment as the within-subject factor and genotype as the between-subjects factor. Statistical comparisons of biochemical analysis results were performed using two-way ANOVA followed by Fisher's least significant difference post hoc test. Statistical comparisons of correlations were performed using Spearman's rho test. Results are expressed as mean ± standard error of mean of control samples; *p*-values <0.05 were considered statistically significant.

3. Results

To study the effects of intranasal insulin in the AD brain, we used the APP/PS1 mouse model and age-matched WT littermates. After intranasal insulin or saline treatment, the mice underwent FDG-PET imaging to assess glucose metabolism in different brain regions. Subsequently, the spatial memory of the mice was analyzed using the Morris swim task after intranasal insulin or saline administration. With some exceptions, the same animals underwent FDG-PET and spatial memory testing twice, with intranasal insulin or saline treatment, and were then divided into intranasal insulin or saline groups before sacrificing. The timeline of the FDG-PET imaging and spatial memory testing is illustrated in Figure 1. To study the biochemical effect of intranasal insulin, the brain regions of interest were collected and homogenized.

3.1. Moderately increased glucose uptake in FDG-PET in ventral brain regions after intranasal insulin in WT mice as compared with APP/PS1 mice

The effect of intranasal insulin treatment on glucose uptake was determined separately for the olfactory bulb, cerebellum, and ventral half of the remaining brain using anatomical boundaries by FDG-PET imaging (Fig. 2A). In addition, the hippocampal voxels were extracted using an Atlas-based template for quantification of hippocampal FDG uptake. The main insulin effect on FDG uptake was nonsignificant ($F_{1,13} = 2.2$, $p = 0.17$). The effect approached significance in the ventral brain ($F_{1,13} = 4.2$, $p = 0.06$; Fig. 2B) but was nonsignificant in other brain regions (hippocampus, $p = 0.08$; cerebellum, $p = 0.11$; olfactory bulb, $p = 0.54$). There was no statistically significant main effect of genotype ($p > 0.26$ in all brain regions).

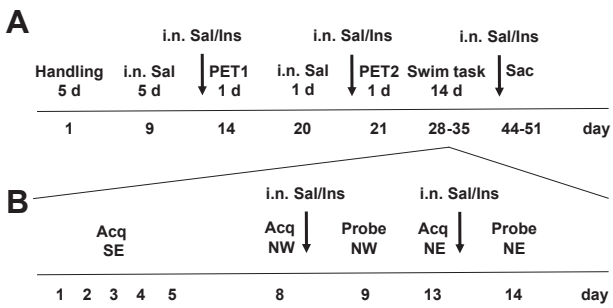

Fig. 1. Timeline of the intranasal insulin treatment study in WT and APP/PS1 mice. (A) The sequence of procedures during the study is shown above the timeline with indicated duration in days (d) for each procedure. The numbers below the timeline denote the start days of each procedure. (B) Detailed description of the Morris swim task. The task began with 5 days of acquisition of the first platform position (SE). A new platform position (NW) was introduced on day 8, and the memory was tested with a probe without platform on day 9. Similarly, another new platform position was introduced on day 13 (NE), followed by a probe test on day 14. The arrows denote administration of intranasal saline or insulin 4 hours before PET imaging on days 14 and 21 (A) as well as after 5 trials of task acquisition on days 8 and 13 (B). Indices: i.n. = intranasal, Sal = saline, Ins = insulin, Acq = acquisition. Abbreviations: PET, positron emission tomography; WT, wild type.

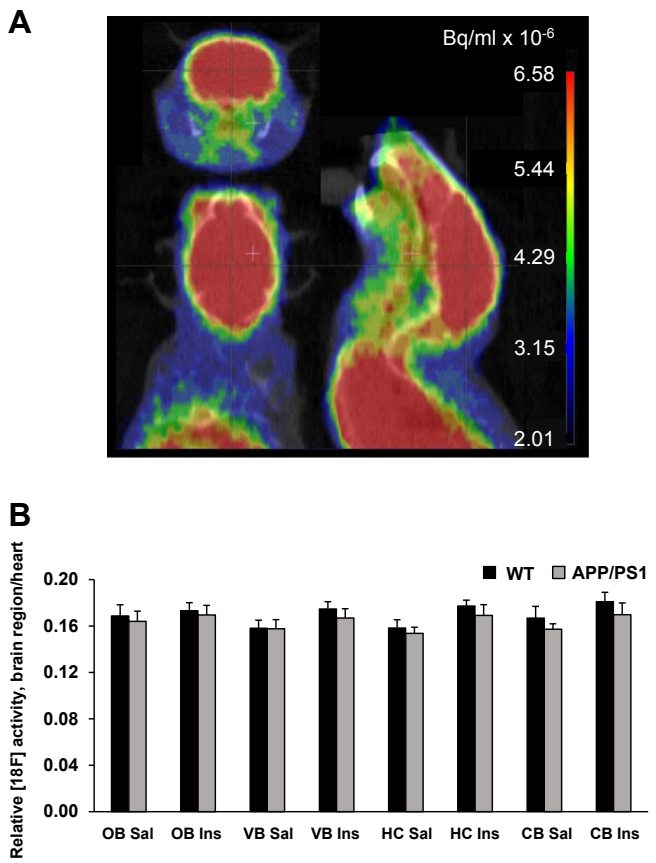

Fig. 2. FDG-PET imaging shows a stronger insulin response in the WT mouse ventral brain and hippocampus than in APP/PS1 mice. (A) FDG-PET image showing accumulated [18F] activity of a mouse head shown in 3 different projections (coronal, horizontal, and sagittal). The scale on the right indicates accumulated [18F] activity in Bq/mL. (B) Relative [18F] activity (brain region/heart) analyzed in the olfactory bulb (OB), ventral brain (VB), hippocampus (HC), and cerebellum (CB) of saline- and insulin-treated WT or APP/PS1 mice shows a stronger insulin effect in the WT mouse VB ($p = 0.06$) and HC ($p = 0.08$) than in APP/PS1 mice. Indices: Sal = saline, Ins = insulin. Results are shown as mean + SEM. n = 7–9, Paired-sample *t*-test. Abbreviations: FDG-PET, [18F]fluoro-2-deoxy-2-D-glucose positron emission tomography; WT, wild type.

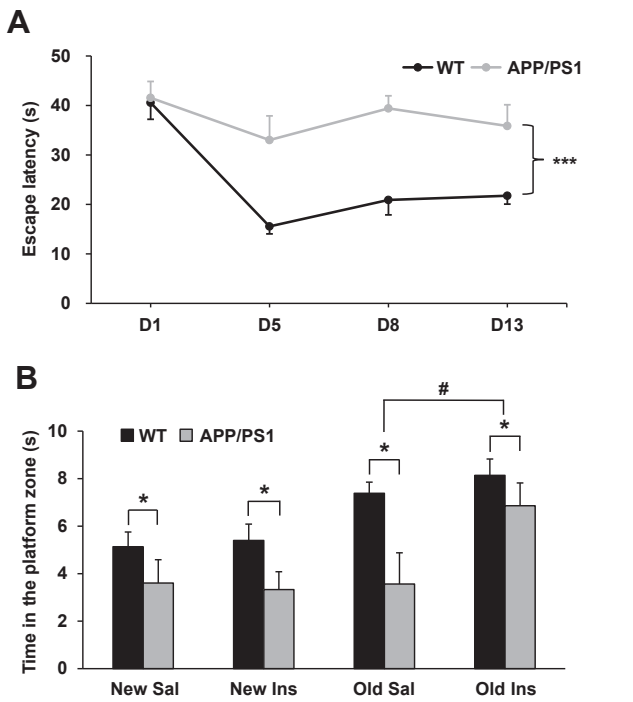

Fig. 3. Significant genotype difference between WT and APP/PS1 mice with a moderate insulin effect on spatial learning in the Morris swim task. (A) Summary of task acquisition during the original platform position (day 1–5), the first new position (day 8), and the second new position (day 13). ***APP/PS1 transgenic mice show longer escape latencies across all phases of the task ($p < 0.001$). (B) Effect of postacquisition intranasal insulin on remembering the newly learned platform position 24 hours later. Indices: New = time in the current target platform zone, Old = time in the original target platform zone, Sal = saline, Ins = insulin. *Significant difference between the genotypes ($p < 0.05$). #Significant effect of insulin treatment ($p < 0.05$). All results are shown as mean + SEM. n = 10–11, ANOVA-RM. Abbreviations: ANOVA-RM, analysis of variance for repeated measures; WT, wild type.

3.2. Postacquisition intranasal insulin impairs spatial memory retention overnight in both WT mice and APP/PS1 mice

Here, our aim was to test whether a single intranasal dose of insulin given after the acquisition period affects encoding and consolidation of a discrete memory (unique platform location) in mice. At all stages of task acquisition (learning the initial platform location on days 1–5, as well as learning a new location on day 8 and day 13), it took longer for APP/PS1 mice to find the escape platform than for WT mice ($F_{1,19} = 21.2$, $p < 0.001$; Fig. 3A). On the other hand, the genotypes did not differ in their swimming speed ($F_{1,19} = 0.5$, $p = 0.47$). After learning a new platform location on day 8 or day 13, the mice were given intranasal insulin or saline, and their memory retention for the newly learned versus original (days 1–5) platform location was tested in a 60-second probe trial without the platform on days 9 and 14. There was no main effect of postacquisition insulin on remembering the newly learned platform location 24 hours later ($F_{1,19} = 0.0$, $p = 1.0$; Fig. 3B). In contrast, the genotype main effect was statistically significant, so that APP/PS1 mice spent less time in the new platform zone ($F_{1,19} = 6.0$, $p = 0.02$; Fig. 3B). On the other hand, WT mice spent also more time in the original platform zone than APP/PS1 mice ($F_{1,16} = 7.5$, $p = 0.01$; Fig. 3B). Intranasal insulin further increased the time in the original platform zone, more clearly for APP/PS1 mice, but also for WT mice, so that the main treatment effect became significant ($F_{1,16} = 6.6$, $p = 0.02$; Fig. 3B). Importantly, intranasal insulin had no effect on the swimming speed ($F_{1,19} = 0.1$, $p = 0.73$), speaking against any systemic hypoglycemic effect of the treatment. These findings suggest that a single intranasal dose of insulin given right after the learning session impairs memory retention at least when assessed 24 hours later.

3.3. Insulin treatment activates Akt2 in the WT, but not in the APP/PS1 mouse hippocampus

Because intranasal insulin treatment showed the most prominent effect on glucose uptake in FDG-PET in the ventral brain regions, including the hippocampus, we next focused on the hippocampus to elucidate the role of Akt kinases, central mediators in the insulin signaling pathway, in this process. The olfactory bulb was used as an insulin nonresponsive control region. To investigate the activation of Akt kinases, we assessed the level of the phosphorylation of Akt1 and Akt2 at the serine 473 and serine 474 residues, respectively, in hippocampal lysates of WT and APP/PS1 mice treated with intranasal insulin or saline. Phosphorylation at these sites leads to activation of the Akt kinase activity. Insulin treatment did not affect the phosphorylation level of Akt1 at serine 473 residue in either the olfactory bulb ($F_{1,14} = 1.7$, $p = 0.21$; Fig. 4A) or the hippocampus ($F_{1,14} = 0.1$, $p = 0.79$; Fig. 4A). However, increased total levels of Akt1 protein (phosphorylated + non-phosphorylated) were observed in the olfactory bulb of both saline-

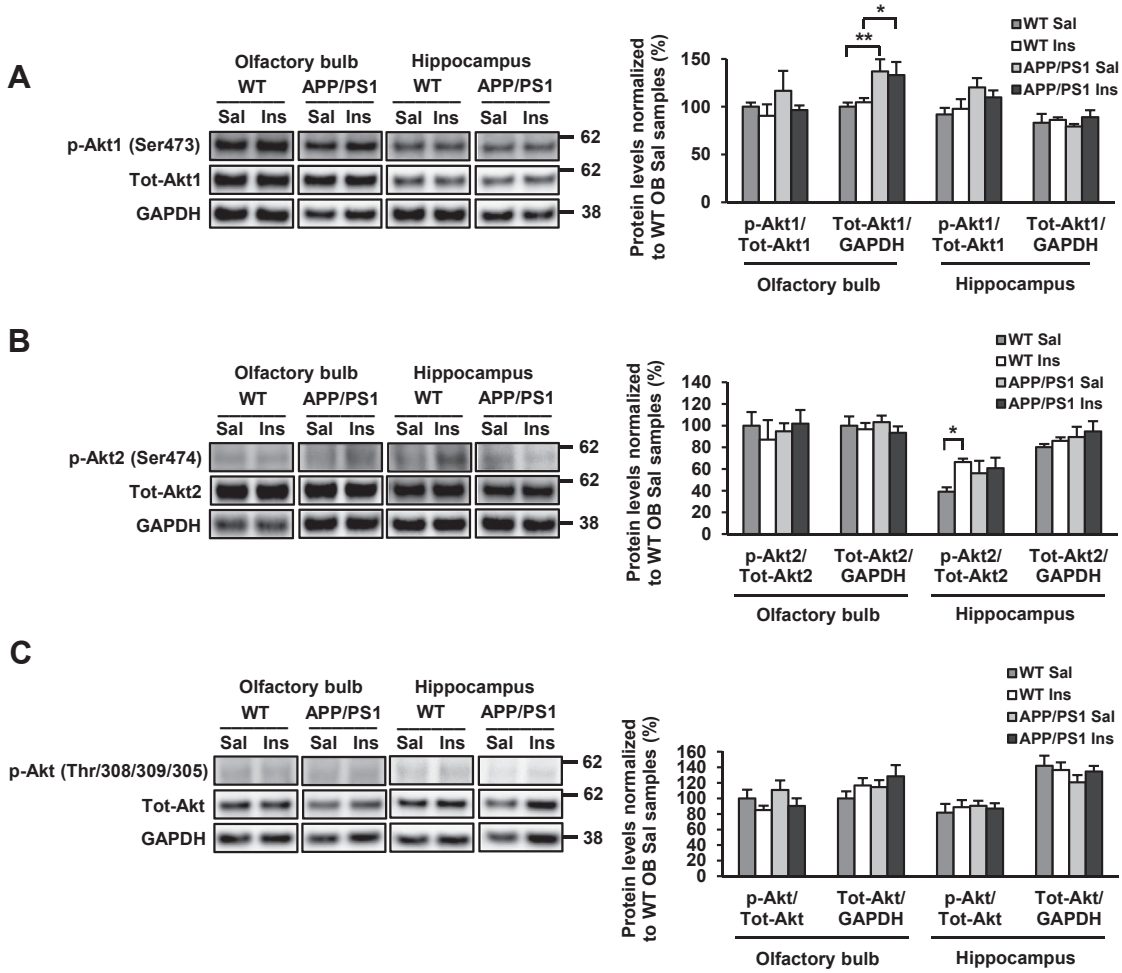

Fig. 4. Insulin treatment specifically increases the activity of Akt2 in the hippocampus of WT, but not APP/PS1 mice. (A) Western blot analysis of the olfactory bulb (OB) and hippocampus of WT and APP/PS1 mice treated with saline (Sal) or insulin (Ins) showed that insulin had no effect on the phosphorylation level of Akt1 at serine 473 (Ser473). Total Akt1 levels were increased in the olfactory bulb of both saline- and insulin-treated APP/PS1 mice as compared to WT mice. (B) Insulin treatment moderately increased the phosphorylation of Akt2 at serine 474 (Ser474) in the WT hippocampus, but not in the APP/PS1 hippocampus. (C) Phosphorylation levels of the threonine 308 and 309 (Thr308/309/305) sites in Akt1, Akt2, and Akt3, respectively, were not altered after insulin treatment in either brain area. Phosphorylated protein levels were normalized to their respective total protein levels in cell lysates, and total protein levels were normalized to those of GAPDH in each sample. All results are shown as mean % + SEM of WT OB Sal. n = 4–5, two-way ANOVA, post hoc LSD. $^{*}p < 0.05$, $^{**}p < 0.01$. Abbreviations: ANOVA, analysis of variance; LSD, least significant difference; WT, wild type.

and insulin-treated APP/PS1 mice as compared with WT mice ($F_{1,14} = 10.6$, $p = 0.006$; Fig. 4A). Interestingly, insulin treatment increased the phosphorylation of Akt2 at serine 474 residue by ~70% in the WT mouse hippocampus, but not in the APP/PS1 mouse hippocampus (Fig. 4B). No treatment effect was seen ($F_{1,14} = 2.1$, $p = 0.17$). However, when 2 obvious outliers (1 in saline and 1 in insulin group) were removed in the APP/PS1 group of mice, the treatment main effect became statistically significant ($F_{1,12} = 11.1$, $p = 0.006$). We also analyzed the phosphorylation status of Akt1 and Akt2 at other phosphorylation sites regulating Akt kinase activity at threonine 308 and 309 residues, respectively (this antibody does not differentiate between the Akt isoforms). However, insulin treatment did not affect the phosphorylation status of Akt1 or Akt2 at threonine 308 or 309 in either the olfactory bulb ($F_{1,14} = 2.9$, $p = 0.11$; Fig. 4C) or the hippocampus ($F_{1,14} = 0.04$, $p = 0.85$; Fig. 4C).

3.4. The levels of autophagosomal markers p62 and LC3-I are altered on insulin treatment in the WT, but not in the APP/PS1 mouse hippocampus

After the observation that insulin treatment specifically activated Akt2 in the hippocampus of WT mice (Fig. 4B), we wanted to study the downstream effects of Akt2 activation. We analyzed the phosphorylation levels of GSK3β at the inhibitory serine 9 residue and tau protein at the serine 202 and threonine 205 and serine 208 residues in the hippocampal lysates of WT and APP/PS1 mice treated with intranasal saline or insulin. Insulin treatment did not affect the phosphorylation status of GSK3β at Ser9 inhibitory residue in the hippocampus of WT or APP/PS1 mice ($F_{1,15} = 2.2$, $p = 0.16$; Fig. 5A). However, we observed a significant genotype effect ($F_{1,15} = 8.4$, $p = 0.01$), such that the phosphorylation levels of GSK3β at Ser9 were 36% lower in the insulin-treated APP/PS1 hippocampus than in the insulin-treated WT hippocampus (Fig. 5A). Total GSK3β protein levels were significantly elevated by ~30% in the hippocampus of APP/PS1 as compared to WT mice in both saline- and insulin-treated groups ($F_{1,15} = 22.7$, $p < 0.001$; Fig. 5A). Insulin treatment had no significant main effect on phosphorylation of tau protein in the hippocampus ($F_{1,15} = 0.1$, $p = 0.72$; Fig. 5B) when using an antibody detecting phosphorylated Ser202, Thr205, and Ser208 residues in tau. However, there was a significant genotype × treatment interaction, such that insulin decreased phosphorylated tau levels in WT mice but increased those in APP/PS1 mice ($F_{1,15} = 5.0$, $p = 0.04$; Fig. 5B). In addition, owing to the intimate link between Akt and mammalian target of rapamycin complex 1

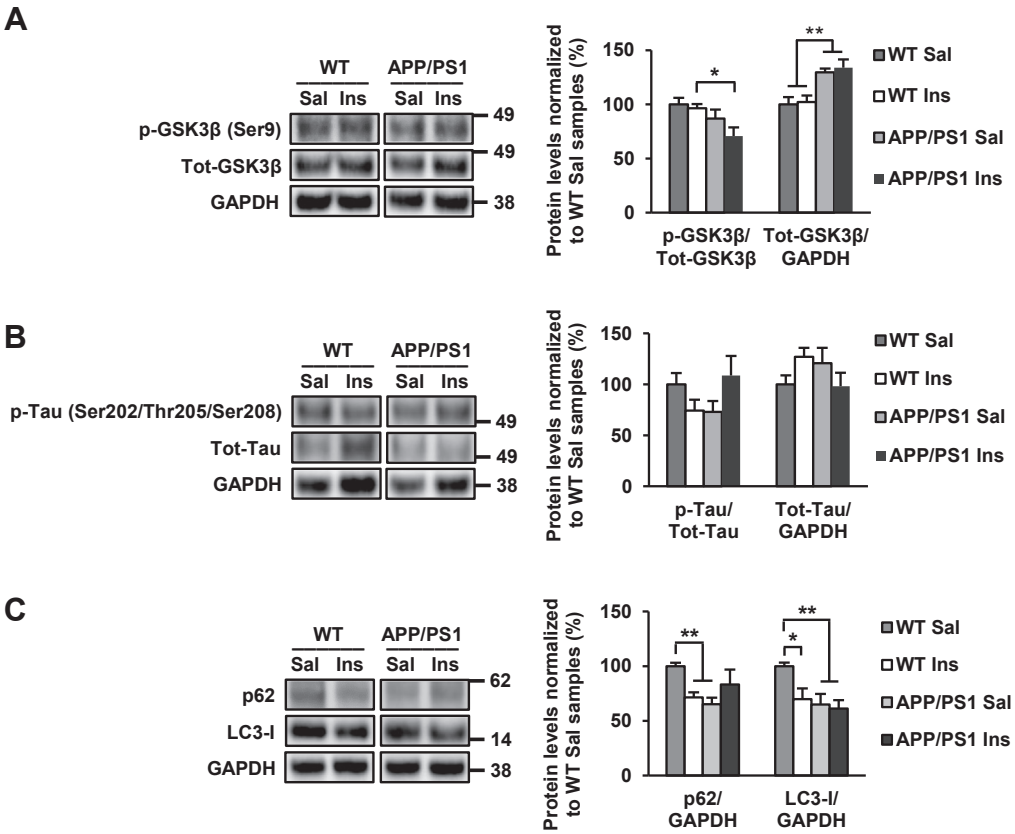

Fig. 5. The levels of autophagosomal markers p62 and LC3-I are decreased on insulin treatment in the hippocampus of WT, but not APP/PS1 mice. (A) Western blot analysis of the WT and APP/PS1 mouse hippocampus showed no significant changes in the phosphorylation level of GSK3β at serine 9 (Ser9) between saline (Sal)- and insulin (Ins)-treated samples. However, the phosphorylation levels of GSK3β were significantly lower in the insulin-treated APP/PS1 hippocampus than in the WT hippocampus. In addition, there were significantly elevated total GSK3β levels in the APP/PS1 hippocampus as compared to the WT hippocampus in both saline- and insulin-treated groups. (B) Insulin treatment had no significant effect on tau phosphorylation in the hippocampus of WT or APP/PS1 mice. (C) The protein levels of autophagosomal markers p62 and LC3-I were significantly lower in the hippocampus of APP/PS1 mice than WT mice on saline treatment. Furthermore, p62 and LC3-I levels were significantly decreased in the hippocampus on insulin treatment in WT, but not in APP/PS1 mice. Phosphorylated protein levels were normalized to their respective total protein levels in cell lysates, and total protein levels were normalized to those of GAPDH in each sample. All results are shown as % of WT Sal. n = 4–5, mean + SEM, two-way ANOVA, post hoc LSD. $^{*}p < 0.05$, $^{**}p < 0.01$. Abbreviations: ANOVA, analysis of variance; GSK3β, glycogen synthase kinase 3β; LSD, least significant difference; WT, wild type.

(mTORC1) signaling (Caccamo et al., 2018), we next investigated whether insulin treatment affected the levels of autophagosomal markers p62 and LC3 in the hippocampus of WT and APP/PS1 mice treated with intranasal saline or insulin. There was a significant genotype × treatment interaction in p62 levels ($F_{1,13} = 6.6$, $p = 0.02$) such that saline-treated APP/PS1 mice showed lower p62 levels than WT mice, but no genotype difference was found among insulin-treated animals (Fig. 5C). Conversely, insulin treatment decreased p62 levels on average by 30% in WT mice but had no effect in APP/PS1 mice. LC3-I levels were lower in APP/PS1 mice than WT mice ($F_{1,12} = 7.3$, $p = 0.02$), and insulin tended to decrease LC3-I levels in both genotypes ($F_{1,12} = 4.4$, $p = 0.06$) (Fig. 5C).

3.5. FDG uptake correlates with the Akt2 activity in the WT, but not in the APP/PS1 mouse hippocampus

Because intranasal insulin treatment increased both FDG uptake and the phosphorylation levels of Akt2 in serine 474 in the WT mouse hippocampus (Figs. 2B and 4B), we next investigated the possible correlation between these results. As expected, there was a significant positive correlation between FDG uptake and Akt2 phosphorylation levels in the hippocampus of saline- or insulin-treated WT (n = 6, r = 0.94, $p = 0.005$; Fig. 6A) but not in

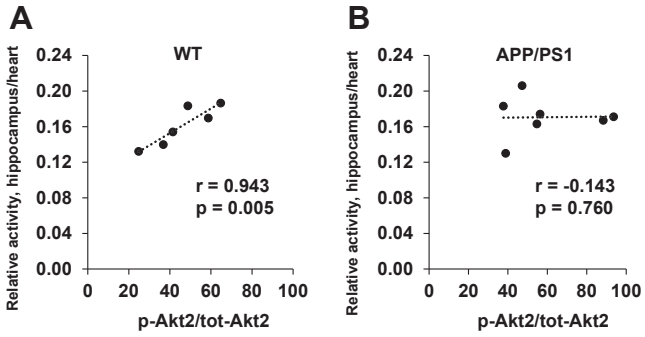

Fig. 6. Akt2 phosphorylation correlates with glucose uptake in the WT, but not in APP/PS1, mouse hippocampus. The correlation analysis of WT (A) or APP/PS1 (B) mice treated with saline or insulin revealed a significant correlation between FDG uptake and Akt2 phosphorylation levels in the WT hippocampus (n = 6, r = 0.94, $p = 0.005$), but not in the APP/PS1 hippocampus (n = 7, r = −0.14, $p = 0.76$). FDG uptake was assessed using PET imaging. Accumulated [18F] activity (Bq/mL) in the hippocampus was normalized to accumulated activity in the heart, and results are shown as relative activity. Akt2 phosphorylation levels were analyzed using Western blotting. Phosphorylated protein levels were normalized to total Akt2 protein levels and are shown as % of the levels in WT Sal samples. Abbreviations: FDG, [^{18}F]fluoro-2-deoxy-2-D-glucose; PET, positron emission tomography; WT, wild type.

APP/PS1 mice (n = 7, r = −0.14, $p = 0.76$; Fig. 6B). In addition, we found a significant positive correlation between Akt2 (Ser474) and GSK3β (Ser9) phosphorylation levels in the hippocampus of insulin-treated WT and APP/PS1 mice (n = 9, r = 0.67, $p = 0.049$, data not shown). In addition, a significant negative correlation between Akt2 (Ser474) and tau (Ser202, Thr205, and Ser208) phosphorylation levels was observed (n = 9, r = −0.78, $p = 0.013$, data not shown). In contrast, there was no significant correlation between the phosphorylation levels of Akt1 and GSK3β in the hippocampus of insulin-treated WT and APP/PS1 mice (n = 9, r = −0.38, $p = 0.31$, data not shown). Finally, a significant negative correlation between GSK3β and tau phosphorylation levels in the hippocampus was observed in insulin-treated WT and APP/PS1 mice (n = 9, r = −0.67, $p < 0.05$, data not shown).

3.6. Intranasal insulin differentially affects the expression of homeostatic microglia markers in the hippocampus of WT and APP/PS1 mice

Apart from regulating GSK3β by inhibitory phosphorylation, Akt2 inhibits FoxO1, which is a transcription factor known to be a key regulator of endogenous glucose production (Latva-Rasku et al., 2017). To investigate the transcriptional response of FoxO1 to insulin treatment, we analyzed the expression levels of 3 known target genes of FoxO1, namely, *Rictor*, *Sestrin3* (*Sesn3*), and *Pak1* (Chen et al., 2010; de la Torre-Ubieta et al., 2010), in the hippocampus of WT and APP/PS1 mice. The expression levels of *Rictor* ($F_{1,15} = 15.6$, $p = 0.001$) and *Sesn3* ($F_{1,16} = 12.7$, $p = 0.003$) showed a significant genotype × treatment interaction, such that their expression levels were reduced on insulin treatment in the WT hippocampus but increased in the APP/PS1 hippocampus (Fig. 7A). The expression of *Pak1* followed the same trend as the expression of *Rictor* and *Sesn3*, although this change was not statistically significant ($F_{1,16} = 4.1$, $p = 0.06$; Fig. 7A). In addition to this, we wanted to investigate the expression of homeostatic (*P2ry12* and *Cx3cr1*) and DAM markers (*Trem2, Tyrobp* and *Cst7)* (Keren-Shaul et al., 2017) as well as astrocytic (*Gfap*) and neuronal (*Bdnf)* markers in the hippocampus of WT and APP/PS1 mice, and their response to intranasal insulin treatment (Fig. 7B and C). The mRNA levels of homeostatic microglia markers *P2ry12* and *Cx3cr1* were significantly higher in the insulin-treated APP/PS1 mice than the insulin-treated WT mice (Fig. 7B). The expression levels of both *P2ry12* ($F_{1,16} = 18.0$, $p < 0.001$) and *Cx3cr1* ($F_{1,17} = 16.1$, $p < 0.001$) showed a significant genotype effect. There was also a significant genotype × treatment interaction with *P2ry12* ($F_{1,16} = 8.1$, $p = 0.01$), but not with *Cx3cr1* ($F_{1,17} = 2.2$, $p = 0.16$). Although the expression of DAM markers *Trem2, Tyrobp,* and *Cst7* was significantly increased ($F_{1,16} = 132.0$, $p < 1 \times 10^{-8}$; $F_{1,16} = 183.1$, $p < 1 \times 10^{-9}$; $F_{1,16} = 241.0$, $p < 1 \times 10^{-10}$, respectively) in APP/PS1 mice as compared to WT mice, no statistically significant changes were observed between insulin- and saline-treated WT or APP/PS1 mice (Fig. 7C). Similarly, increased expression of *Gfap* in APP/PS1 mice as compared to WT mice ($F_{1,15} = 165.1$, $p < 1 \times 10^{-8}$) was observed, but insulin treatment per se did not affect the expression of *Gfap* or *Bdnf* in the hippocampus of WT or APP/PS1 mice (Fig. 7D).

4. Discussion

In this study, we have investigated how intranasal insulin treatment modulates glucose uptake, Akt signaling cascade, the phosphorylation status of Tau protein, autophagy, and the expression of glial and neuronal markers in WT and APP/PS1 mice.

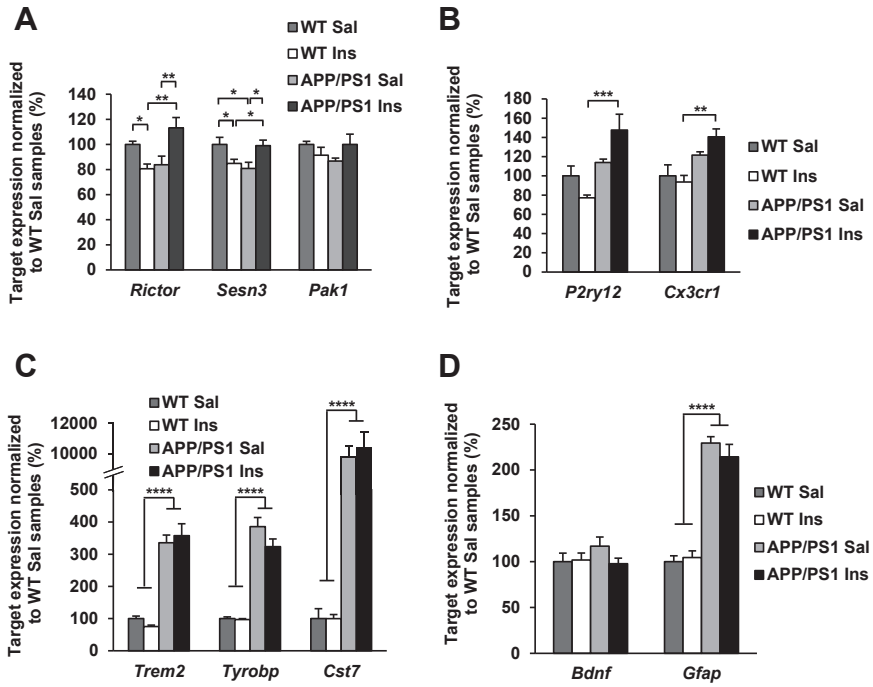

Fig. 7. Intranasal insulin affects differentially the expression of FoxO1-regulated target genes and homeostatic microglia markers in the hippocampus of WT and APP/PS1 mice. (A) RT-qPCR analysis of the hippocampus of WT and APP/PS1 mice treated with saline (Sal) or insulin (Ins) showed that insulin treatment significantly downregulated *Rictor* and *Sestrin3* (*Sesn3*) in the WT hippocampus. In contrast, these target genes were significantly upregulated in the APP/PS1 hippocampus in response to intranasal insulin treatment. *Pak1* expression followed a similar trend. Basal expression levels of all 3 genes were lower in the APP/PS1 hippocampus than in the WT hippocampus. (B) The mRNA levels of homeostatic microglia markers *P2ry12* and *Cx3cr1* were significantly higher in the hippocampus of insulin-treated APP/PS1 mice than insulin-treated WT mice. (C) The mRNA levels of disease-associated microglia markers *Trem2*, *Tyrobp*, and *Cst7* were significantly upregulated in the hippocampus of APP/PS1, but not WT mice. (D) The mRNA analysis of astrocytic (*Gfap*) and neuronal (*Bdnf*) markers in the hippocampus of APP/PS1 and WT mice. Gene expression levels were normalized to those of *Gapdh* and are shown as % of WT Sal. n = 4–6, mean + SEM, two-way ANOVA, post hoc LSD. $^{*}p < 0.05$, $^{**}p < 0.01$, $^{***}p < 0.001$, $^{****}p < 0.0001$. Abbreviations: ANOVA, analysis of variance; LSD, least significant difference; WT, wild type.

Furthermore, we assessed how this treatment affects spatial learning and memory in these mice. We also for the first time delineated the specific involvement of Akt1 and Akt2 in the hippocampus on intranasal insulin treatment. FDG-PET imaging showed that insulin treatment increased glucose uptake in the ventral brain and hippocampus of WT mice, but not APP/PS1 mice. In the Morris swim task, we observed that WT mice learned the first location of the platform and subsequently found the new platform locations significantly faster than APP/PS1 mice. However, intranasal insulin treatment delayed the learning of new platform locations of both WT and APP/PS1 mice. We also found out that intranasal insulin treatment specifically activated Akt2, but not Akt1, in the hippocampus of WT mice, whereas a similar effect was not observed in APP/PS1 mice. Consistent with the insulin effect on the activation of Akt2 signaling, insulin treatment decreased the transcriptional activity of FoxO1, a downstream target of Akt2, and a key regulator of endogenous glucose production (Latva-Rasku et al., 2017). This was shown by significantly lower expression levels of FoxO1-regulated target genes *Rictor* and *Sesn3* in the hippocampus of WT mice, but not in APP/PS1 mice. Thus, our results suggest that on intranasal insulin treatment, Akt2 is specifically activated in the hippocampus of WT mice, which in turn coincides with the increased uptake of FDG and altered FoxO1-mediated gene expression in the hippocampus. Importantly, these changes did not take place in the hippocampus of APP/PS1 mice, suggesting a disadvantageous link between AD-associated genetic background and insulin-induced Akt2 signaling in the brain. Also, the observations that intranasal insulin differentially affected the expression of homeostatic microglia markers *P2ry12* and *Cx3cr1* and the levels of autophagosomal markers p62 and LC3-I between APP/PS1 and WT mice suggest diverse cellular responses for insulin in the brain tissue depending on the degree of AD-related pathology.

Previous studies have assessed changes in Akt levels in the context of brain insulin signaling without assessing the contribution of the individual Akt subtypes (Stanley et al., 2016; Takeda et al., 2010). Here, we show that Akt2 is the Akt family member, which is specifically activated on intranasal insulin treatment in the healthy mouse brain. This is an interesting finding as the key role of Akt2 in glucose metabolism is supported by population-based studies in humans demonstrating that individuals carrying the *AKT2* P50T genetic variant have on average a 40% reduction in glucose uptake in the whole body (Latva-Rasku et al., 2017). We observed that the insulin-induced activation of Akt2 was associated with an increased phosphorylation status at serine 474 residue known to be phosphorylated by mTORC2, but not at threonine 308/309/305, which are phosphorylated by PDK1. It should be noted, however, that we cannot completely rule out the possibility that insulin might also activate Akt2 via threonine 309 as the antibody used detects phosphorylated threonine 308/309/305 residues in all Akt1, Akt2, and Akt3 isoforms, respectively, and thus the effect on Akt2 may be masked. Previous studies have demonstrated a more robust insulin effect on Akt phosphorylation in the mouse hypothalamus (Takeda et al., 2010) and hippocampus (Stanley et al., 2016). However, these studies have either used genetically obese leptin-deficient mice (Takeda et al., 2010), which have reduced Akt phosphorylation levels in the hippocampus and cortex (Clodfelder-Miller et al., 2005), or delivered insulin directly into the hippocampus via reverse microdialysis (Stanley et al., 2016). Although insulin receptors are found in the olfactory bulb (Duarte et al., 2012), we did not observe insulin-related effects in the olfactory bulb of WT or APP/PS1 mice. These findings are consistent with a recent study in aged rats, showing significant metabolic effect of acute intranasal insulin in the ventral brain, excluding the olfactory bulb (Anderson et al., 2017).

In addition to regulating glucose metabolism, insulin has been shown to play a key role in neuronal development, neurotransmission, neuroprotection, and learning and memory (Duarte et al., 2012). However, it should be emphasized that not all studies have reported positive effects of intranasal insulin treatment on memory (Chapman et al., 2017). This may derive from variations in the dose that reaches the critical brain region (which is difficult to estimate) and also from the timing of the administration. Our aim here was to test whether a single dose of intranasal insulin given after the acquisition period affects encoding and consolidation of a discrete memory (unique platform location) in mice. Testing 24 hours after the insulin treatment did not find evidence for enhanced spatial memory. Rather, mice in the insulin group remembered better the original platform location than the new platform locations during the task acquisition phase than the saline-treated mice. This suggests that insulin might have impaired memory related to the most recent platform location. Interestingly, a recent study in aged rats under similar test conditions revealed that a single intranasal dose of insulin given on the test day (24 hours since learning) did not improve memory recall (Anderson et al., 2017). In general, the most beneficial effects of intranasal insulin have been obtained with repetitive dosing (Chapman et al., 2017), suggesting involvement of slowly developing metabolic or biochemical processes in insulin effects. Recent studies have found that insulin promotes dendritic spine and synapse formation in rat hippocampal primary neuron cultures (Lee et al., 2011). However, we did not find changes in *Bdnf* expression levels in the hippocampus of insulin- or saline-treated middle-aged WT or APP/PS1 mice, suggesting that a single dose of intranasal insulin did not induce a marked neurotrophic response. This is consistent with the lack of positive insulin effect on spatial memory, but most likely not the only underlying mechanism that remains to be disclosed in future studies.

Downstream of Akt2 signaling, the FoxO-Pak1 transcriptional pathway regulates neuronal polarity (de la Torre-Ubieta et al., 2010). Akt2 inhibits the transcription factor FoxO1 by phosphorylating it, after which FoxO1 translocates from the nucleus to the cytosol (Dong, 2018). Here, we observed a moderate downregulation of *Pak1*, a target gene of FoxO1, in response to insulin treatment in the hippocampus of WT mice, but not in APP/PS1 mice, reinforcing the idea of impaired insulin signaling pathways in APP/PS1 mice. Insulin-induced PI3K-Akt-mTOR pathway is also closely linked to autophagosomal regulation (Caccamo et al., 2018), and the rapamycin-mediated mammalian target of rapamycin (mTOR) inhibition has been shown to decrease the levels of $A\beta_{42}$ in the hippocampus and consequently ameliorate the memory deficits by increasing autophagy in AD mouse models (Caccamo et al., 2010; Spilman et al., 2010). In the present study, we observed a significant decrease in the levels of autophagosomal markers p62 and LC3-I in the hippocampus on intranasal insulin treatment in WT, but not in APP/PS1 mice. Also, these markers were significantly lower in saline-treated APP/PS1 mice than WT mice, suggesting that their autophagosomal activity was already altered in the basal condition. Because we were unable to detect the phosphatidylethanolamine-conjugated form of LC3 (LC3-II), it is difficult to interpret whether decreased levels of LC3-I reflect increased autophagosomal activity. However, simultaneous reduction of p62 levels on intranasal insulin treatment in WT mice further suggests increased, rather than decreased, autophagosomal activity. This is contrary to what one would expect if Akt activation leads to mTORC1 activation and thereby inhibition of autophagy (Zhou et al., 2018). On the other hand, some reports suggest that Akt phosphorylated at threonine 308, but not at serine 473, is required for mTORC1 activation (Guertin et al., 2006; Rodrik-Outmezguine et al., 2011). We observed here insulin-induced phosphorylation of Akt2

predominantly at serine 474 and not threonine 309 (corresponding to serine 473 and threonine 308 in Akt1).

Apart from the differential activation of Akt2 in the hippocampus of WT and APP/PS1 mice on intranasal insulin treatment, the homeostatic microglia markers, *P2ry12* and *Cx3cr1,* displayed dissimilar expression response between APP/PS1 and WT mice on insulin treatment. However, the expression analysis of the astrocytic marker *Gfap* did not reveal prominent insulin-dependent changes. These are important findings given the recent advances in the characterization of a unique microglia type associated with neurodegenerative diseases (DAM) (Keren-Shaul et al., 2017). DAM are regulated through a two-step activation mechanism in the mouse models of AD. In the first step, the increased expression of specific set of genes such as TREM2-signaling adaptor protein (*Tyrobp*) is observed, whereas the homeostatic microglial markers, such as *P2ry12* and *Cx3cr1*, show decreased expression. The second step, which is TREM2-dependent, involves a switch toward increased expression of a specific set of genes, such as *Trem2* and *Cst7*. Importantly, DAM have the potential to restrict neurodegeneration, which emphasizes the importance of assessing the RNA signature of DAM targets on different treatment procedures, which are aimed to modify AD-associated outcome measures. Although intranasal insulin did not affect the expression of DAM target genes, we detected the expected increase of *Trem2*, *Tyrobp*, and *Cst7* expressions in the hippocampus of APP/PS1 mice as compared to WT mice (Ulrich et al., 2018). Importantly, the fact that intranasal insulin increased the expression of both *P2ry12* and *Cx3cr1* in the hippocampus of APP/PS1 mice, but tended to decrease it in WT mice, suggests that intranasal insulin treatment significantly promotes the prevailing homeostatic status of microglia in APP/PS1 mice as compared to WT mice. Thus, it is important in future studies to assess, in a similar experimental setting, the effects of intranasal insulin on the microglia status by, for example, analyzing their activity using PET radiotracers available for microglia. Collectively, these are crucial findings in the context of ongoing intranasal insulin trials targeted against AD and mild cognitive impairment because insulin deficit has been linked intimately to AD-associated neuroinflammation ("Nasal Insulin," n.d.).

Although previous studies with intranasal insulin in humans and rodents have shown generally encouraging results in improving cognition, they have not consistently demonstrated if intranasal insulin treatment ameliorates tau pathology in AD mouse models (Chapman et al., 2017). We did not observe significant changes in the phosphorylation at the inhibitory Ser9 site of the Akt2 downstream target GSK3β, the main kinase phosphorylating tau, in either WT or APP/PS1 mice. In line with this, no changes in tau phosphorylation in these mice were detected. Nevertheless, we found a significant positive correlation between Akt2 (Ser474) and GSK3β (Ser9) phosphorylation levels in the hippocampus of insulin-treated WT and APP/PS1 mice, confirming that increased activation of Akt2 results in inhibition of GSK3β activity. In addition, there was a significant negative correlation between Akt2 (Ser474) and tau (Ser202, Thr205 and Ser208) phosphorylation levels, suggesting that Akt2 activation leads to decreased tau phosphorylation likely through decreased activity of GSK3β (Hooper et al., 2008). These correlations are consistent with insulin-induced activation of Akt2. However, the timing and repetition of the insulin administration appear to crucially affect the results in behavioral testing, in vivo imaging, physiological analysis, and postmortem biochemical analysis (Chapman et al., 2017). We also suspect that while acute insulin treatment increases glucose uptake in the brain, chronic or repeated treatment may be required to achieve trophic effects, such as restoring synaptic plasticity and eventually ameliorating cognition in AD mouse models or patients with AD.

In conclusion, we demonstrate here that intranasal insulin treatment moderately increases glucose uptake in the WT mouse hippocampus via activating the Akt2 signaling pathway. We also suggest that peripheral glucose intolerance in APP/PS1 mice could associate with impaired insulin-induced Akt2 signaling in the brain. Our results highlight the therapeutic potential of intranasally administered insulin as a noninvasive delivery method, which overcomes the blood-brain barrier and reaches the brain at biochemically effective levels. Further studies with chronic intranasal insulin treatment are required to elucidate the downstream effects of Akt2 activation in the hippocampus as well as the potential trophic effects of insulin on recovering synaptic plasticity and enhancing cognition in the AD brain.

Disclosure

The authors have no actual or potential conflicts of interest.

Acknowledgements

This work was funded by Academy of Finland, Finland (grant numbers 288659, 307866 and 315459), Sigrid Jusélius Foundation, European Regional Development Fund project A71429, Neurophenotyping core facility supported by University of Eastern Finland, Finland and Biocenter Finland, Strategic Neuroscience Funding of the University of Eastern Finland, Doctoral Programme in Molecular Medicine at the University of Eastern Finland, and SynaNet consortium funded by the European Union's Horizon 2020 research and innovation programme (grant number 692340). Development of B6 custom antibody was funded by the European Union's Horizon 2020 research and innovation programme (grant agreement 686009). APF was funded by the European Union's FP7 Marie-Curie Initial Training Network programme (grant agreement 606950).

References

Alcantara, D., Timms, A.E., Gripp, K., Baker, L., Park, K., Collins, S., Cheng, C., Stewart, F., Mehta, S.G., Saggar, A., Sztriha, L., Zombor, M., Caluseriu, O., Mesterman, R., Van Allen, M.I., Jacquinet, A., Ygberg, S., Bernstein, J.A., Wenger, A.M., Guturu, H., Bejerano, G., Gomez-Ospina, N., Lehman, A., Alfei, E., Pantaleoni, C., Conti, V., Guerrini, R., Moog, U., Graham Jr., J.M., Hevner, R., Dobyns, W.B., O'Driscoll, M., Mirzaa, G.M., 2017. Mutations of AKT3 are associated with a wide spectrum of developmental disorders including extreme megalencephaly. Brain 140, 2610–2622.

Anderson, K.L., Frazier, H.N., Maimaiti, S., Bakshi, V.V., Majeed, Z.R., Brewer, L.D., Porter, N.M., Lin, A.-L., Thibault, O., 2017. Impact of single or repeated dose intranasal zinc-free insulin in young and aged F344 rats on cognition, signaling, and brain metabolism. J. Gerontol. A. Biol. Sci. Med. Sci. 72, 189–197.

Apostolatos, A., Song, S., Acosta, S., Peart, M., Watson, J.E., Bickford, P., Cooper, D.R., Patel, N.A., 2012. Insulin promotes neuronal survival via the alternatively spliced protein kinase CδII isoform. J. Biol. Chem. 287, 9299–9310.

Baker, L.D., Cross, D.J., Minoshima, S., Belongia, D., Watson, G.S., Craft, S., 2011. Insulin resistance and Alzheimer-like reductions in regional cerebral glucose metabolism for cognitively normal adults with prediabetes or early type 2 diabetes. Arch. Neurol. 68, 51–57.

Bell, G.A., Fadool, D.A., 2017. Awake, long-term intranasal insulin treatment does not affect object memory, odor discrimination, or reversal learning in mice. Physiol. Behav. 174, 104–113.

Benedict, C., Hallschmid, M., Hatke, A., Schultes, B., Fehm, H.L., Born, J., Kern, W., 2004. Intranasal insulin improves memory in humans. Psychoneuroendocrinology 29, 1326–1334.

Benedict, C., Hallschmid, M., Schultes, B., Born, J., Kern, W., 2007. Intranasal insulin to improve memory function in humans. Neuroendocrinology 86, 136–142.

Benedict, C., Kern, W., Schultes, B., Born, J., Hallschmid, M., 2008. Differential sensitivity of men and women to anorexigenic and memory-improving effects of intranasal insulin. J. Clin. Endocrinol. Metab. 93, 1339–1344.

Borchelt, D.R., Ratovitski, T., van Lare, J., Lee, M.K., Gonzales, V., Jenkins, N.A., Copeland, N.G., Price, D.L., Sisodia, S.S., 1997. Accelerated amyloid deposition in the brains of transgenic mice coexpressing mutant presenilin 1 and amyloid precursor proteins. Neuron 19, 939–945.

Brünner, Y.F., Kofoet, A., Benedict, C., Freiherr, J., 2015. Central insulin administration improves odor-cued reactivation of spatial memory in young men. J. Clin. Endocrinol. Metab. 100, 212–219.

Caccamo, A., Belfiore, R., Oddo, S., 2018. Genetically reducing mTOR signaling rescues central insulin dysregulation in a mouse model of Alzheimer's disease. Neurobiol. Aging 68, 59–67.
Caccamo, A., Majumder, S., Richardson, A., Strong, R., Oddo, S., 2010. Molecular interplay between mammalian target of rapamycin (mTOR), amyloid-beta, and Tau: effects on cognitive impairments. J. Biol. Chem. 285, 13107–13120.
Chapman, C.D., Schiöth, H.B., Grillo, C.A., Benedict, C., 2017. Intranasal insulin in Alzheimer's disease: food for thought. Neuropharmacology 136 (Pt B), 196–201.
Chen, C.-C., Jeon, S.-M., Bhaskar, P.T., Nogueira, V., Sundararajan, D., Tonic, I., Park, Y., Hay, N., 2010. FoxOs inhibit mTORC1 and activate Akt by inducing the expression of Sestrin3 and rictor. Dev. Cell 18, 592–604.
Chiu, S.-L., Chen, C.-M., Cline, H.T., 2008. Insulin receptor signaling regulates synapse number, dendritic plasticity, and circuit function in vivo. Neuron 58, 708–719.
Clodfelder-Miller, B., De Sarno, P., Zmijewska, A.A., Song, L., Jope, R.S., 2005. Physiological and pathological changes in glucose regulate brain Akt and glycogen synthase kinase-3. J. Biol. Chem. 280, 39723–39731.
Cohen, A.D., Klunk, W.E., 2014. Early detection of Alzheimer's disease using PiB and FDG PET. Neurobiol. Dis. 72 (Pt A), 117–122.
Craft, S., Baker, L.D., Montine, T.J., Minoshima, S., Watson, G.S., Claxton, A., Arbuckle, M., Callaghan, M., Tsai, E., Plymate, S.R., Green, P.S., Leverenz, J., Cross, D., Gerton, B., 2012. Intranasal insulin therapy for Alzheimer disease and amnestic mild cognitive impairment: a pilot clinical trial. Arch. Neurol. 69, 29–38.
de la Torre-Ubieta, L., Gaudillière, B., Yang, Y., Ikeuchi, Y., Yamada, T., DiBacco, S., Stegmüller, J., Schüller, U., Salih, D.A., Rowitch, D., Brunet, A., Bonni, A., 2010. A FOXO-Pak1 transcriptional pathway controls neuronal polarity. Genes Dev. 24, 799–813.
Dhuria, S.V., Hanson, L.R., Frey, W.H., 2010. Intranasal delivery to the central nervous system: mechanisms and experimental considerations. J. Pharm. Sci. 99, 1654–1673.
Dong, X.C., 2018. SCP4: a small nuclear phosphatase having a big effect on FoxOs in gluconeogenesis. Diabetes 67, 23–25.
Duarte, A.I., Moreira, P.I., Oliveira, C.R., 2012. Insulin in central nervous system: more than just a peripheral hormone. J. Aging Res. 2012, 1–21.
Ganong, W.F., 2000. Circumventricular organs: definition and role in the regulation of endocrine and autonomic function. Clin. Exp. Pharmacol. Physiol. 27, 422–427.
Guertin, D.A., Stevens, D.M., Thoreen, C.C., Burds, A.A., Kalaany, N.Y., Moffat, J., Brown, M., Fitzgerald, K.J., Sabatini, D.M., 2006. Ablation in mice of the mTORC components raptor, rictor, or mLST8 reveals that mTORC2 is required for signaling to Akt-FOXO and PKCα, but not S6K1. Dev. Cell 11, 859–871.
Hanson, L.R., Fine, J.M., Svitak, A.L., Faltesek, K.A., 2013. Intranasal administration of CNS therapeutics to awake mice. J. Vis. Exp. 8.
Hiltunen, M., Khandelwal, V.K.M., Yaluri, N., Tiilikainen, T., Tusa, M., Koivisto, H., Krzisch, M., Vepsäläinen, S., Mäkinen, P., Kemppainen, S., Miettinen, P., Haapasalo, A., Soininen, H., Laakso, M., Tanila, H., 2012. Contribution of genetic and dietary insulin resistance to Alzheimer phenotype in APP/PS1 transgenic mice. J. Cell. Mol. Med. 16, 1206–1222.
Hooper, C., Killick, R., Lovestone, S., 2008. The GSK3 hypothesis of Alzheimer's disease. J. Neurochem. 104, 1433–1439.
Irie, F., Fitzpatrick, A.L., Lopez, O.L., Kuller, L.H., Peila, R., Newman, A.B., Launer, L.J., 2008. Enhanced risk for Alzheimer disease in persons with type 2 diabetes and APOE ε4. Arch. Neurol. 65, 89–93.
Jankowsky, J.L., Fadale, D.J., Anderson, J., Xu, G.M., Gonzales, V., Jenkins, N.A., Copeland, N.G., Lee, M.K., Younkin, L.H., Wagner, S.L., Younkin, S.G., Borchelt, D.R., 2004. Mutant presenilins specifically elevate the levels of the 42 residue β-amyloid peptide in vivo: evidence for augmentation of a 42-specific γ secretase. Hum. Mol. Genet. 13, 159–170.
Keren-Shaul, H., Spinrad, A., Weiner, A., Matcovitch-Natan, O., Dvir-Szternfeld, R., Ulland, T.K., David, E., Baruch, K., Lara-Astaiso, D., Toth, B., Itzkovitz, S., Colonna, M., Schwartz, M., Amit, I., 2017. A unique microglia type Associated with restricting development of Alzheimer's disease. Cell 169, 1276–1290.e17.
Kooistra, M., Geerlings, M.I., Mali, W.P.T.M., Vincken, K.L., van der Graaf, Y., Biessels, G.J., 2013. Diabetes mellitus and progression of vascular brain lesions and brain atrophy in patients with symptomatic atherosclerotic disease. The SMART-MR study. J. Neurol. Sci. 332, 69–74.
Latva-Rasku, A., Honka, M.-J., Stančáková, A., Koistinen, H.A., Kuusisto, J., Guan, L., Manning, A.K., Stringham, H., Gloyn, A.L., Lindgren, C.M., , T2D-GENES Consortium, the T.-G, Collins, F.S., Mohlke, K.L., Scott, L.J., Karjalainen, T., Nummenmaa, L., Boehnke, M., Nuutila, P., Laakso, M., 2017. A Partial Loss-of-function Variant Akt2 Is Associated Reduced Insulin-mediated Glucose Uptake Mult. Insulin Sensitive Tissues: a Genotype-Based Callback Positron Emission Tomography Study. Diabetes 67, 334–342.
Lee, C.-C., Huang, C.-C., Hsu, K.-S., 2011. Insulin promotes dendritic spine and synapse formation by the PI3K/Akt/mTOR and Rac1 signaling pathways. Neuropharmacology 61, 867–879.
Liu, Y., Liu, F., Grundke-Iqbal, I., Iqbal, K., Gong, C.-X., 2011. Deficient brain insulin signalling pathway in Alzheimer's disease and diabetes. J. Pathol. 225, 54–62.
Livak, K.J., Schmittgen, T.D., 2001. Analysis of relative gene expression data using real-time quantitative PCR and the 2(-Delta Delta C(T)) Method. Methods 25, 402–408.
Mao, Y.-F., Guo, Z., Zheng, T., Jiang, Y., Yan, Y., Yin, X., Chen, Y., Zhang, B., 2016. Intranasal insulin alleviates cognitive deficits and amyloid pathology in young adult APPswe/PS1dE9 mice. Aging Cell 15, 893–902.
Moran, C., Phan, T.G., Chen, J., Blizzard, L., Beare, R., Venn, A., Münch, G., Wood, A.G., Forbes, J., Greenaway, T.M., Pearson, S., Srikanth, V., 2013. Brain atrophy in type 2 diabetes: regional distribution and influence on cognition. Diabetes Care 36, 4036–4042.
Mosconi, L., Sorbi, S., de Leon, M.J., Li, Y., Nacmias, B., Myoung, P.S., Tsui, W., Ginestroni, A., Bessi, V., Fayyazz, M., Caffarra, P., Pupi, A., 2006. Hypometabolism exceeds atrophy in presymptomatic early-onset familial Alzheimer's disease. J. Nucl. Med. 47, 1778–1786.
Nasal Insulin [WWW Document]. https://www.alzforum.Org/therapeutics/nasal-insulin. (Accessed 26 October 2018).
Noguchi, M., Suizu, F., 2012. Regulation of AKT by phosphorylation of distinct threonine and serine residues. In: Berhardt, L.V. (Ed.), Advances in Medicine and Biology. Nova Science Publishers, Hauppauge, NY, pp. 139–162. http://www.novapublishers.org/catalog/product_info.php?products_id=35675.
Novak, V., Milberg, W., Hao, Y., Munshi, M., Novak, P., Galica, A., Manor, B., Roberson, P., Craft, S., Abduljalil, A., 2014. Enhancement of vasoreactivity and cognition by intranasal insulin in type 2 diabetes. Diabetes Care 37, 751–759.
Reger, M.A., Watson, G.S., Frey, W.H., Baker, L.D., Cholerton, B., Keeling, M.L., Belongia, D.A., Fishel, M.A., Plymate, S.R., Schellenberg, G.D., Cherrier, M.M., Craft, S., 2006. Effects of intranasal insulin on cognition in memory-impaired older adults: modulation by APOE genotype. Neurobiol. Aging 27, 451–458.
Reger, M.A., Watson, G.S., Green, P.S., Baker, L.D., Cholerton, B., Fishel, M.A., Plymate, S.R., Cherrier, M.M., Schellenberg, G.D., Frey, W.H., Craft, S., Craft, S., 2008. Intranasal insulin administration dose-dependently modulates verbal memory and plasma amyloid-beta in memory-impaired older adults. J. Alzheimers. Dis. 13, 323–331.
Rodrik-Outmezguine, V.S., Chandarlapaty, S., Pagano, N.C., Poulikakos, P.I., Scaltriti, M., Moskatel, E., Baselga, J., Guichard, S., Rosen, N., 2011. mTOR kinase inhibition causes feedback-dependent biphasic regulation of AKT signaling. Cancer Discov. 1, 248–259.
Salameh, T.S., Bullock, K.M., Hujoel, I.A., Niehoff, M.L., Wolden-Hanson, T., Kim, J., Morley, J.E., Farr, S.A., Banks, W.A., 2015. Central nervous system delivery of intranasal insulin: mechanisms of uptake and effects on cognition. J. Alzheimer's Dis. 47, 715–728.
Shah, K., Desilva, S., Abbruscato, T., 2012. The role of glucose transporters in brain disease: diabetes and Alzheimer's Disease. Int. J. Mol. Sci. 13, 12629–12655.
Spilman, P., Podlutskaya, N., Hart, M.J., Debnath, J., Gorostiza, O., Bredesen, D., Richardson, A., Strong, R., Galvan, V., 2010. Inhibition of mTOR by rapamycin abolishes cognitive deficits and reduces amyloid-β levels in a mouse model of Alzheimer's disease. PLoS One 5, e9979.
Stanley, M., Macauley, S.L., Caesar, E.E., Koscal, L.J., Moritz, W., Robinson, G.O., Roh, J., Keyser, J., Jiang, H., Holtzman, D.M., 2016. The effects of peripheral and central high insulin on brain insulin signaling and amyloid-β in young and old APP/PS1 mice. J. Neurosci. 36, 11704–11715.
Steen, E., Terry, B.M., Rivera, E.J., Cannon, J.L., Neely, T.R., Tavares, R., Xu, X.J., Wands, J.R., de la Monte, S.M., 2005. Impaired insulin and insulin-like growth factor expression and signaling mechanisms in Alzheimer's disease – is this type 3 diabetes? J. Alzheimer's Dis. 7, 63–80.
Takalo, M., Haapasalo, A., Martiskainen, H., Kurkinen, K.M.A., Koivisto, H., Miettinen, P., Khandelwal, V.K.M., Kemppainen, S., Kaminska, D., Mäkinen, P., Leinonen, V., Pihlajamäki, J., Soininen, H., Laakso, M., Tanila, H., Hiltunen, M., 2014. High-fat diet increases tau expression in the brain of T2DM and AD mice independently of peripheral metabolic status. J. Nutr. Biochem. 25, 634–641.
Takeda, S., Sato, N., Uchio-Yamada, K., Sawada, K., Kunieda, T., Takeuchi, D., Kurinami, H., Shinohara, M., Rakugi, H., Morishita, R., 2010. Diabetes-accelerated memory dysfunction via cerebrovascular inflammation and Abeta deposition in an Alzheimer mouse model with diabetes. Proc. Natl. Acad. Sci. U.S.A. 107, 7036–7041.
Ulrich, J.D., Ulland, T.K., Mahan, T.E., Nyström, S., Nilsson, K.P., Song, W.M., Zhou, Y., Reinartz, M., Choi, S., Jiang, H., Stewart, F.R., Anderson, E., Wang, Y., Colonna, M., Holtzman, D.M., 2018. ApoE facilitates the microglial response to amyloid plaque pathology. J. Exp. Med. 215, 1047–1058.
van Elderen, S.G.C., de Roos, A., de Craen, A.J.M., Westendorp, R.G.J., Blauw, G.J., Jukema, J.W., Bollen, E.L.E.M., Middelkoop, H.A.M., van Buchem, M.A., van der Grond, J., 2010. Progression of brain atrophy and cognitive decline in diabetes mellitus: a 3-year follow-up. Neurology 75, 997–1002.
Vanhanen, M., Soininen, H., 1998. Glucose intolerance, cognitive impairment and Alzheimer's disease. Curr. Opin. Neurol. 11, 673–677.
Vannucci, S.J., Koehler-Stec, E.M., Li, K., Reynolds, T.H., Clark, R., Simpson, I.A., 1998. GLUT4 glucose transporter expression in rodent brain: effect of diabetes. Brain Res. 797, 1–11.
Xu, W.L., von Strauss, E., Qiu, C.X., Winblad, B., Fratiglioni, L., 2009. Uncontrolled diabetes increases the risk of Alzheimer's disease: a population-based cohort study. Diabetologia 52, 1031–1039.
Zhao, W.-Q., Townsend, M., 2009. Insulin resistance and amyloidogenesis as common molecular foundation for type 2 diabetes and Alzheimer's disease. Biochim. Biophys. Acta 1792, 482–496.
Zhou, Y., Ulland, T.K., Colonna, M., 2018. TREM2-Dependent effects on microglia in Alzheimer's disease. Front. Aging Neurosci. 10, 202.